

The Reflection By An Ionized Meteor Trail From Remote Station To Radio Signal Receiver In Malaysia.

¹Shahrizan Bin Mohd Razali, Zulkarnaen bin Mohd Lajin & Mohd Fauzi B. Ali

¹shahrizan@psis.edu.my , Politeknik Sultan Idris Shah

Abstract

This research discusses the implementation of a radio receiver to receive signals from a remote station that result from reflection by an ionized meteor trail. The receiver is situated in Batu Pahat, Johor (1° 52'U, 103° 07' T) while the transmitter is Stesen Pemancar Radio Perlis fm, Pauh (6°09'U, 1009 26' T). The transmitter is chosen based on its operating frequency and power, and distance from the receiver. This radio receiver system consists of a six element Yagi Antenna, a 10 dB pre amplifier, a commercial analogue radio and a personal computer equipped with a Spectrogram. The specifications of the Yagi antenna are made based on the characteristics of the transmitter and the signals' propagation distance between both transmitter and receiver. The antenna is simulated and optimized using the Quick Yagi and 4NEC2x. Then it is tested and such parameters like VSWR, gain and radiation characteristics are measured and compared with the value from simulation. Since the antenna's gain does not meet the requirement, a pre amplifier is designed. The pre amplifier uses a voltage divider topology with common-emitter configuration. The pre amplifier is attached to a commercial radio that is connected to a personal computer. The characteristic of the propagating signal is analyzed to estimate the optimum elevation angle of the antenna from the horizon. Finally, it is tested on the peak of α -Capricornids (3 July 2017 – 15 August 2017) meteor showers. However, the display not recorded because of technical error that is recording error and bad weather within rain. Therefore, the test will be done on 12 August 2017 where at time Perseids meteor shower. Therefore, the objective of the project is achieved theoretically and practically.

Keywords: Meteor, Transmitter, Receiver, Yagi-Uda, amplifier

Introduction

A communication systems using meteor scatter meteor's ionized tail bouncing radio waves to enable it to be accepted as far as 2,000 kilometers (km) from the transmitter. The first monitoring was reported by professionals in the mid-1930s. Several studies have been listed by the non-professional in about the 1960s and 1970s, but the approach was made using a computer in the 1980s, which has given over a long period by a group of amateurs to monitor the project (Reddy & Premkumar, 2018). At about 1988, satellite system has been questioned in which the effect of the existence of new technologies advanced and sophisticated such as microprocessor and makes the scientists took the approach of using the reflection of the effect of scattering meteor and provides higher frequencies as a backup resistance to the system output -height. Recognizing the potential and usefulness to communication systems and benefits of meteor in the military field, Oetting, through his journal has made observations to each point of distribution of meteor with the aim of increasing the success of any military mission (Sulimov, 2017; Oetting, 1980). In addition, the usage of meteor communication is also very useful in obtaining data by using the remote control system that requires an extensive network and remote. A

sprinkling of meteors has some other potential benefits for high frequency applications that are commonly used in digital communication over long distances. In the communication system in the present high frequencies which require more locations and frequency management day by day, during the day, and at the time of use frequency maximum in the ionosphere and density as well as interference in many lines can be reduced by controlling the communication network meteor itself. Thus it can help the efficiency of the communication system. (Reddy & Premkumar, 2018; Sulimov, 2017; Wakabayashi, 2020)

Natural phenomena can be applied in a communication system by comprising signal transmission and reception of radio waves in the distance of 200 km to 2000 km from the transmitter through reflection by the tail of ionized meteor trails that cross the Earth's atmosphere. A simple principle shown meteor scatter communications in Figure 1 (Wakabayashi, 2020). the tail is produced when a meteoroid orbits intersect Earth's orbit Earth's gravitational pull causes the meteoroid entering the earth's atmosphere at a speed of 71 kilometers per second (km / s). When it enters the atmosphere

collide and rub against each other with the ionized air molecules. The ionized meteoroid known as a meteor. Genesis meteors can be classified into two meteor showers and meteor spores. (Wakabayashi, 2020) Table 1 shows the major meteor activity during 2017. In the event of a meteor shower, the rate of formation of the solid state of the tail (the tail of ionized density is below 2×10^{14} electrons / meter) is much slower. Then the probability to receive signals is higher. This is important as a reflection occurs mainly when a radio frequency higher than the frequency of the ionized plasma tail. At the bottom of the solids which radio frequencies lower than the frequency of the ionized plasma tail, the probability of receiving signal is small. However, not all signals can be reflected in the solid state. This depends on the geometry and position of the transmitter-receiver meteor. Meteor scatter communications with proven cost effective for exploiting natural natural occurrence. It also does not depend on the state of the ionosphere to propagate than insensitive to interference phenomena of solar and galactic others. However, it is highly critical of the distance of propagation and reception system environment (Jurgen Rendtel, 2017).

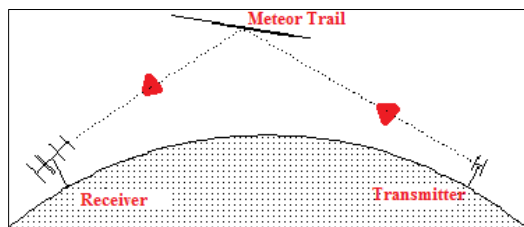


Figure 1: the principle of meteor scatter
[<http://www.imo.net/radio/intro>]

From Table 1 shows the types of meteor showers, the occurrence date and the date of maximumly applicable to get the best time to make observations in the year 2017. However, these experiments only focused on the areas that are shaded to make observations (Jurgen Rendtel, 2017; Yavuz, 1990)

Table 1: 2017 meteor shower

Meteor Shower	Date	Maximum
Quadrantids	28 December – 12 January	4 January
γ -Normids	25 Februari – 28 Mac	14 Mac
η -Aquariids	19 April – 28 May	5 May
η -Lyrids	3 May – 14 May	8 May
Daytime Arietids	22 may -2 July	7 Jun

June Boötids	22 Jun – 2 July	27 Jun
Piscis Austrinids	15 July – 10 August	28 July
Southern δ -Aquariids	12 July – 23 August	30 July
α -Capricornids	3 July – 15 August	30 July
Perseids	17 July – 24 August	12 August
Aurigids	28 August – 5 September	31 August
September ϵ -Perseids	5 September – 21 September	9 September
Daytime Sextantids	9 September – 9 Oktober	27 September
Southern Taurids	10 September – 20 November	10 Oktober
δ -Aurigids	10 Oktober – 18 Oktober	11 Oktober
Phoenicids	28 November – 9 December	2 December
Ursids	17 December – 26 December	2 December

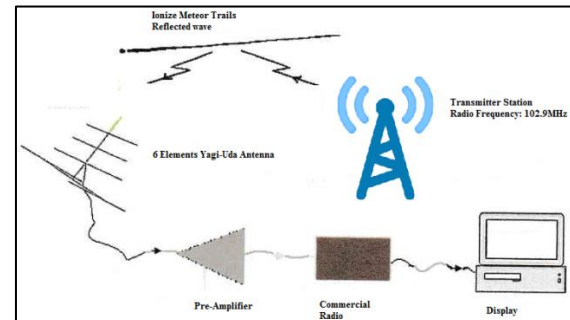


Figure2: Overall receiver system

Receiver system that would be built is shown in Figure 2. However, before it can be built, a transmission station selected in advance. Then from the analysis of signal propagation distance, the antenna is built and tested to determine whether the signal that would be received at a level that is optimal or not. If there is a partial amplifier is required. In the final, observation of the signal is made. Existing commercial radio is used for the purpose of tuning and demodulating the signal while the computer containing the software Spectrogram 12 used to observe, store and analyze the signals. (Oetting, 1980)

Objectives

The objective of this study is to develop a system and helps to identify the meteors activity located near to the equator. In addition, it works to develop appropriate tools to enable it to operate in the range of very high frequency (VHF) of 102.9MHz. It is very important to understand the way in which the signal is reflected and received a paramount objective to gain knowledge. In addition, it is also important to identify the appropriate software for analysis for every designed equipment.

Analysis

Transmitter

The desired advanced features signal is a single operating frequency 102.9MHz. Power Beam minimized 1kW and a transmitter and receiver for at least 200 km. Thus the existing transmission stations is selected. Information on these base stations presented in Table 4.1

Table 4.1 Information of Transmitter station (H, 2017).

Name of transmitting station	Perlis FM Transmitter
Position	6 ° 09'U. 100 ° 26 'E
Height	1217 meters from sea level
transmitter height	80 meters
Overall height	1297 meters
Frequency	102.9MHz
Power transmission	4.5dBi/2kW

Distance Between Transmitter With Receiver (approximate) Ranking antenna driver is (6 ° 09'U, 100 ° 26 '1), and the receiving antenna in Kg Parit Raja (1 ° 52'U, 103 ° 07' E). Receiver antenna height from sea level is 25 meters.

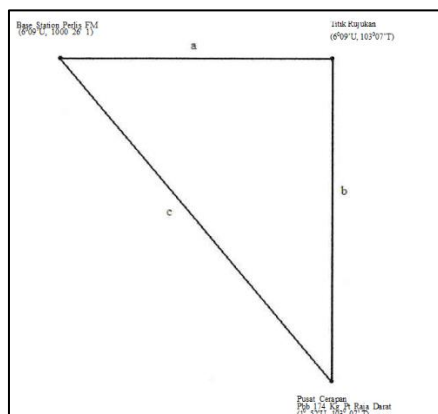


Figure 4.1: Position of transmitter and receiver stations (Ince, 1980; McKinley, 1961)

Figure 4.1 on the results obtained from informal discussions with one of the employees of the Department of Survey and Mapping Malaysia (JUPEM). The distance between base stations with the reference point is represented by 'a' is 294 km while the distance between the reference point for Parit Raja is represented by 'b' is 432 km. From the diagram above, the vertical distance between the transmitter station Perlis FM receiver locations are represented by 'c' is using the following formula: (Jayaram, 2021; McKinley, 1961)

$$c = \sqrt{a^2 + b^2} = \sqrt{294^2 + 432^2} = 523km$$

Antenna alignment angles are: -

$$\theta = \tan^{-1} a/b = \tan^{-1} 294/4320 = 34.2^\circ$$

From the above calculation, the vertical distance is 523 km and the tilt angle of the antenna is 34.2° west. If the signal is transmitted directly from the transmitting antenna to the receiving antenna the maximum distance between two antennas regardless of wave reflection are (McKinley, 1961):

$$d = \sqrt{2hr} + \sqrt{2ht} = \sqrt{2(4256)} + \sqrt{2(82)} = 105.1 \text{ feet} = 169km$$

Reflection angle

With the use of high frequency 102.9MHz then the average radio signal reflection is:

The average echo height of meteor is given by (McKinley, 1961):

$$H = -17 \log_{10} f + 124 = -17 \log_{10} 102.9MHz + 124 = 89.79km$$

The overall height of the reflection of radio signals from Earth's surface is 89.79km. This value is added to the value obtained after the height of the transmitter antenna. Based on the calculation, available vertical height of the 89.79km of the earth's surface, a layer of the ionosphere: Suitable used in the coating layer E. The maximum value of the electron density of 1.5×10^{11} elektrton / m³

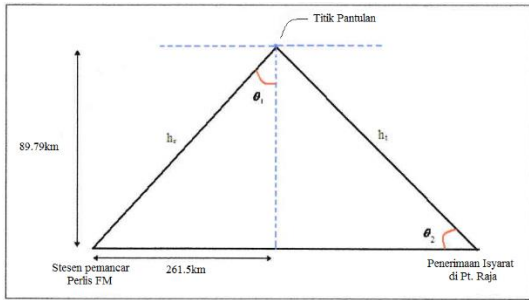


Figure 4.3: Model of propagation of the signal wave (fig calculation) (McKinley, 1961)

Figure 4.3: Model of propagation of the signal wave (fig calculation) Parameter values obtained in the above calculation is based on the figure 4.1. 261.5km value obtained as a result of the $c / 2$

Figure 4.2:

$$\text{Reflection angle } \theta_1 = \tan^{-1} \left[\frac{261.5}{89.79} \right] = 71.05^\circ$$

Critical frequency

$$f_{crit} = 9\sqrt{N_{max}} = 9\sqrt{1.5 \times 10^{11}} = 3.49 \text{ MHz}$$

Maximum usable frequency

$$MUF = \left[\frac{f_{crit}}{\cos \theta} \right] = \frac{3.49}{\cos 71.05^\circ} = 10.75 \text{ MHz}$$

Optimum working frequency $OWF = 80\% \times MUF = 0.8 \times 10.75 = 8.60 \text{ MHz}$

Tilt angle of acceptance

$$\theta = 180^\circ - 90^\circ - 71.05^\circ = 18.95^\circ$$

Distance signal propagation

$(h_r + h_t), h_r = h_t = 2\sqrt{261.5^2 + 89.79^2} = 2 \times 276.49 = 552.97 \text{ km}$. The curvature of the Earth taken into account

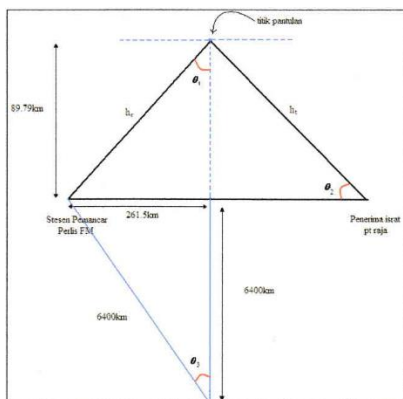


Figure 4.4: Digital signal propagation wave

By using the equation of an equilateral triangle (McKinley, 1961):-

$$h_r^2 = 6400^2 + (6400 + 89.79)^2 - (2 \times 6400 \times (6400 + 89.79) \times \cos 2.34^\circ) = 77330.89$$

$$h_r = 278.08 \text{ km}$$

Therefore, by using the law of the triangle is obtained

$$\left[\frac{6400}{\sin \theta_1} \right] = \left[\frac{h_r}{\sin 2.34^\circ} \right]$$

$$\sin \theta_1 = \frac{(6400 \times \sin 2.34^\circ)}{278.08}$$

$$\theta_1 = 70^\circ$$

Thus, the, $MUF = f_{crit} / \cos \theta = 3.19 / \cos 70^\circ = 10.20 \text{ MHz}$

While $OWF = 80\% \times MUF = 8.16 \text{ MHz}$

the angle of tilt receiver $\theta_2 = 180^\circ - 90^\circ - 70^\circ = 20^\circ$

The distance signal propagation $(h_r = h_t = 2 \times 278.08 = 556.16 \text{ km}$

Maximum Reflection Angle:

From Figure 4.4 The maximum angle of reflection can be reflected by the ionosphere is through the following formula (McKinley, 1961): -

$$\theta = \sin^{-1} \left[\frac{R}{R + H} \right] = \sin^{-1} \left[\frac{6400}{6400 + 89.79} \right] = 80.45^\circ$$

The maximum distance between transmitter and receiver is caused by the reflection of the ionosphere $-d = 2 \times \tan 80.45^\circ \times 89.79 = 2 \times 533.70 = 1067.4 \text{ km}$

Power calculation

It is known that the gain of the transmitter is 4.5dBi while the recipient is a 28dBi antenna gain (antenna gain + gain of the amplifier). By assuming the loss of power at the transmitter and receiver is 1dB, then the total power at the receiving antenna can be calculated using the following formula (McKinley, 1961):

$$P_r = P_t - L_t + G_t - L_b + G_r - L_r$$

Therefore Total transmitter power is

$$10 \log_{10} 2000 = 33.0 \text{ dBW}$$

Loss of power in free air space (L_b) is

$$20 \log_{10} D + 20 \log_{10} f + 32.4 = 20 \log_{10} 523 + 20 \log_{10} 102.9 + 32.4 = 127.02 \text{ dB}$$

$$\begin{aligned} \text{Power receiver } (P_r) \text{ is } P_r &= P_t - L_t + G_t - L_b + G_r - L_r \\ &= 33 \text{ dBW} - 1 \text{ dB} + 4.5 \text{ dBi} - 127.02 \text{ dB} + 28 \text{ dBi} - 1 \text{ dB} \\ &= -63.52 \text{ dBW} = -33.52 \text{ dBm} \end{aligned}$$

Receiver antenna

Specifications for this study is the antenna operating frequency = 102.9MHz, driver lengths $L_1 = 1.458m$, long director $D_3 = 1.385$, reflectors lengths $L_2 = 1.531m$ 531m long and the distance between elements = 0.12λ . wavelength antenna $\lambda = c/f = 3 \times 10^8 / 102.9 \text{ MHz} = 2.9155$.

The length of the driver is $L_1 = \lambda/2 = 1.4578m$.

$$\begin{aligned} \text{The length of each directors is } D_1 - \frac{5}{100} \times D_1 &= D_2(m), D_2 - \frac{5}{100} \times D_2 = D_3(m), D_3 - \frac{5}{100} \times D_3 = D_4(m) \text{ dan } D_4 - \frac{5}{100} \times D_4 = D_5(m). \end{aligned}$$

The lengths of reflectors $L_R = L_1 + L_1 \frac{5}{100} = 1.5306m$. (Stutzman, W. L., & Thiele, G. A., 2012).

Table 4.2 shows how the antenna is the best choice. From the table, 6 element antenna is the best with a gain of 9.24dB, the ratio of front to rear lobe was 16.38dB and enter the impedance of $16.2 + j31.5$. it is said to be good because of other readings, the gain obtained in yagi 6 element antenna is high, the ratio of front to rear is also high and the length of each pile fastener element is low.

To ensure the experiments and the reading obtained is correct, the gain graph plots is plotted against the number of elements. The result is shown as diagram 4.5. diagram 4.5 shows also where the range between the gain is only 5dB to 15dB only. After 15dB graph shows no improvement occurs. From there it can be concluded that the calculations and the correct choice of antenna is the same as saying that such a theory. (McKinley, 1961; Stutzman, W. L., & Thiele, G. A., 2012).

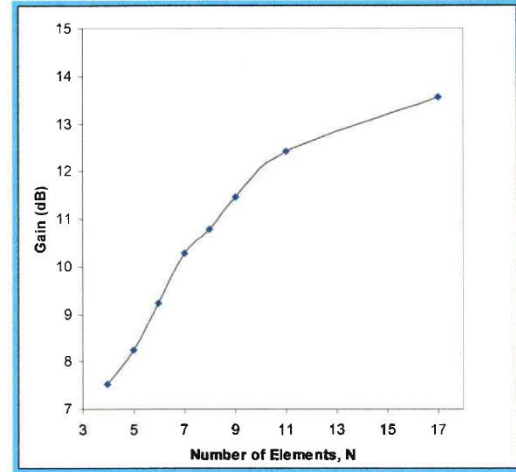


Figure 4.5: The gain against the number of antenna elements.

Table 4.2: 8 Yagi-Uda antenna type separate built to select a set of optimum antenna (Yagi-Uda.com, 2011; Jones, E. A., & Joines, W. T., 1997)

$d/\lambda = 0.0274$ $S_D = 0.2\lambda$	Boom Length of Yagi-Uda Array							
	1.05	1.40	1.75	2.10	2.45	2.80	3.50	5.60
Length of reflector, L_R/λ	0.5238	0.5238	0.5238	0.5138	0.5238	0.5138	0.5138	0.5138
D_1	1.3839	1.3839	1.3839	1.3839	1.3839	1.3839	1.3839	1.3839
D_2	1.3147	1.3147	1.3147	1.3147	1.3147	1.3147	1.3147	1.3147
D_3		1.2490	1.2490	1.2490	1.2490	1.2490	1.2490	1.2490
D_4			1.1866	1.1866	1.1866	1.1866	1.1866	1.1866
D_5				1.1273	1.1273	1.1273	1.1273	1.1273
D_6					1.0709	1.0709	1.0709	1.0709
D_7						1.0174	1.0174	1.0174
D_8							0.9665	0.9665
D_9							0.9182	0.9182
D_{10}								0.8723
D_{11}								0.8287
D_{12}								0.7873
D_{13}								0.7479
D_{14}								0.7105
D_{15}								0.6750
Spacing Between Directores (S_D/λ)	0.12	0.12	0.12	0.12	0.12	0.12	0.12	0.12
Gain (dB)	7.53	8.25	9.24	10.27	10.78	11.46	12.42	13.56
Front-to Back Ratio, DB	16.94	14.08	16.38	22.87	25.87	20.50	20.60	19.30
Input Impedance (Ohm)	15.7+ j43.1	25.0+ j33.2	16.2+ j31.5	13.9+ j34.7	17.5+ j34.7	17.5+ j34.7	15.9+ j34.5	16.4+ j34.5

Input impedance seen by the VSWR. Two readings taken on the oscilloscope signal level. First, the polarity of the oscilloscope under normal conditions, (vi) and second inverted

$$(V_r). \text{ VSWR} = \frac{(V_i + V_r)}{(V_i - V_r)} = 1.03.$$

VWSR is the ratio of the voltage wave in which to make antenna design ideal in all situations (height) of bandwidth. Frequency antenna in accordance often fluctuate based on where it is placed. For example, the value of VSWR = 1 and the corresponding frequency is 102.9MHz and its antenna must height of 10 meters. If the position is changed to 20 meters, then the corresponding frequency will be shifted either forward or backward or not they are worth 102.9MHz. therefore when the antenna VSWR is ideal for Yagi-Uda antenna is valued at between 1.0 to 1.1. (Stutzman, W. L., & Thiele, G. A., 2012).

Yagi antenna elements

As already described, yagi antenna consists of antenna elements that are arranged in parallel, linear and composed of elements of bipolar cylindrical (Glover, 1991). In yagi antenna, there is only one driving element or elements of the receiver which is connected to the transmission line. This element serves to receive power from the transmitter and is one of the most active element in the antenna system. These elements can be either of the dual half-wave dipole, gamma adjustment and other materials that can be adapted to the parasitic elements. Yagi antenna elements can be made of aluminum, copper or alloy. Rate resistivity of each material is different and this affects the efficiency of an antenna. Table 4.3 shows the materials that can be used. (Yagi-Uda.com, 2011)

From Table 4.3 of the selected element in this study is an aluminum rod. Besides it is easily available, it's cheap and easy to operate. Compared to copper, aluminum is much lighter and easier to cut and molded. Similarly, the optimum resistivity when compared with other types of rod. The diameter of the aluminum rod type has been set which is worth 8mm diameter as the supply for other scarce in stores. Furthermore diameter rod will affect the gain and the ratio back to the front lobe. So he made up during the simulation.

Table 4.3: Types of materials for rod antenna element

Materials	Resistivity * $\mu\Omega$	The depth of the skin $+\mu m$ at 1GHz
Aluminium	2.62	2.576
brass (66% copper, 34% zinc)	7.5	4.3586
Copper	1.7241	2.0898
Gold	2.44	2.4861

iron	9.71	4.9594
Nickel	6.9	4.1807
silver	1.62	2.0257
alloy	13-22	5.7384-7.465
can	11.4	5.3737
Titanium	47.8	11.0036

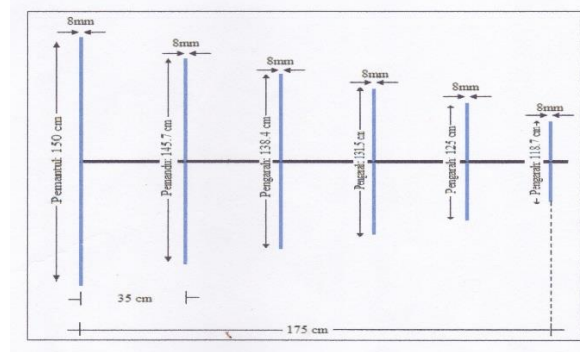


Figure 4.6: Dimensions 6 element yagi antenna receiver (Yagi-Uda.com, 2011)

Antenna measurement

Antenna measurement was tested as in figure 4.7 and 4.8 to ensure that it can work well. The parameters taken into consideration is the input impedance, gain and radiation pattern of the antenna. Some of the tools used:

Signal generators Rohde & Schwartz SMHU
100kHz – 4320MHz
Pensanalisa Spektrek Hewlet Packard 8593E
Osiloskop TDS 220 100MHz

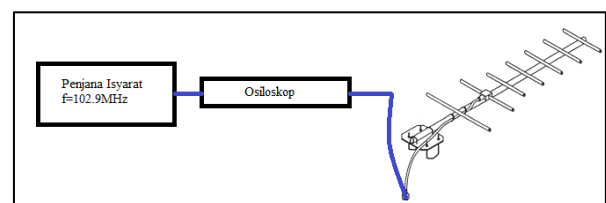


Figure 4.7: The layout for the measurement of antenna impedance input

A viewed through a VSWR impedance. Two readings on the oscilloscope signal level is taken: first, with the polarity of the oscilloscope under normal conditions, (V_i) and the second, inverted, (V_r) (Stutzman, W. L., & Thiele, G. A., 2012).

$$VSWR = \frac{(V_i + V_r)}{(V_i - V_r)} = 1.03$$

VSWR is the ratio of the voltage waveform where the hardcore is important to make the antenna design is ideal in all situations (height) of bandwidth. Frequency antenna often fluctuate

based on where it is placed. For example, the value of $VSWR = 1$ and the corresponding frequency is 102.9MHz and its antenna must be in the height of 10 meters. If the position is changed to 20 meters then the corresponding frequency will be shifted either forward or backward or not they are worth 102.9MHz. Therefore when the antenna VSWR is ideal for Yagi-Uda antenna is valued at between 1.0 to 1.1. (Stutzman, W. L., & Thiele, G. A., 2012; Silver, S. (Ed.), 1984)

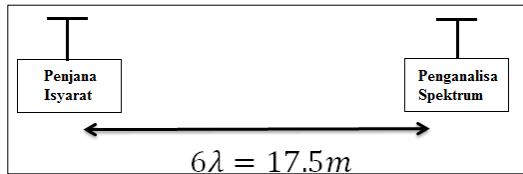


Figure 4.8: The layout of the measurement antenna gain and radiation pattern

The gain was measured by comparing the value obtained with a value of the reference antenna. Yagi antenna gain is 6.2dBi. The radiation pattern is obtained by rotating the antenna 180o and take readings for each 10o. considered symmetric radiation pattern. The plot is as shown in Figure 4.9

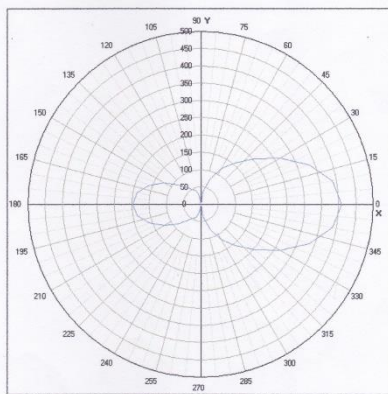


Figure 4.9: Measurement of Radiation Pattern

The radiation pattern obtained has a relatively large lateral and posterior lobes compared to the simulation. However, the radiation pattern is still radiant.

Partial amps (design and testing)

The field strength at the receiver is given by (Stutzman, W. L., & Thiele, G. A., 2012).

$$e = \frac{[173\sqrt{P_1}]}{d} = \frac{[173\sqrt{2k}]}{400k} = 97.21dB\mu Vm^{-1}$$

Out on the field strength and antenna gain measured field strength of the entire existing system is $97.21 dB\mu Vm^{-1}$. While this is sufficient to apply a

radio receiver, a pre-amplifier is required to repair the noise and the received signal quality. This is because commercial analogue radio receivers require multiple antennas at least 10dB. Pre-amplifier topology built using a voltage divider with a common emitter. This is because it is the most stable layouts that are not influenced by multiple factors, leakage currents and temperature. Assuming $V_{BE}=0.7V$ and the transistor qualify $\beta R_E \geq 10R_2$ analysis is made.

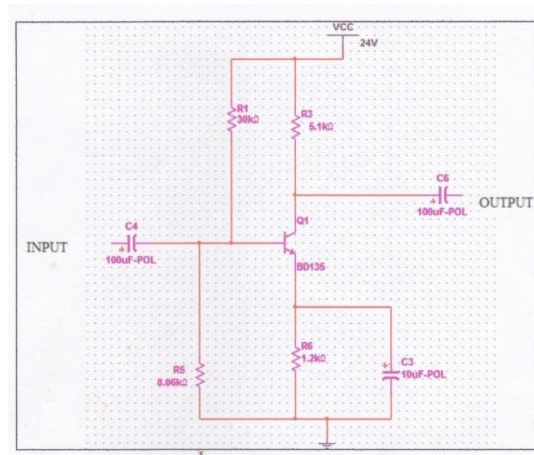


Figure 4.10: Connection Amplifier Circuit 102.9MHz (Poza, D. M., 2000)

Workbench Multisim software simulation results as shown in Figure 10.4 gives the gain is 20dB for frequency 102.9MHz. Figure 4.11 shows the connections made and the gain versus frequency graph obtained. Workbench software has flaws that can be detected that the reading is not fixed and varies each time a new simulation is made. However the real value is not so important as their objective this amplifier is just to get multiples in excess of 10dB (Reddy, M. P., 2018; Poza, D. M., 2000).

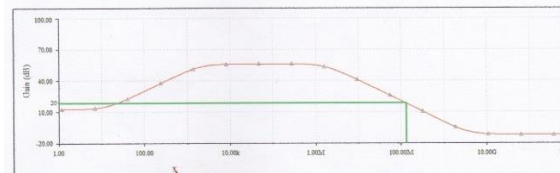


Figure 4.11 gain versus frequency graph of simulation results workbench

When tested in accordance with the layout diagrams 4:12 found pre amplifier gain is 11dB at frequencies around 100MHz to 110MHz. This is quite different with the simulation results. However, pre-amplifier circuit can be used as a multiple of the input radio is 18dB (antenna gain + gain amplifier) that is in excess of 10dB. (The minimum required). The plot of log frequency versus gain for pre-amplifier is shown in Figure 4.13.

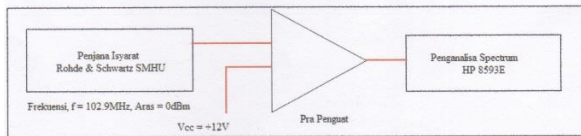


Figure 4.12 Pre amplifier measurement

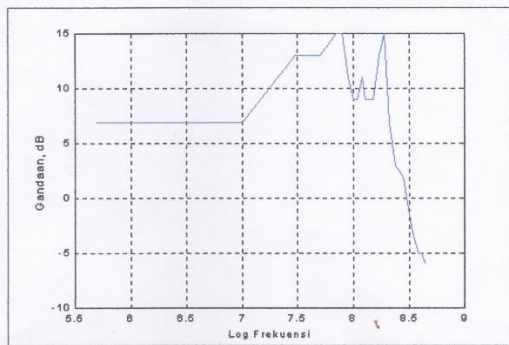


Figure 4.13 Pre-Amplifier Gain Versus Frequency Log

Installation and receiver

The block diagram of the receiving system is shown in Figure 2. Yagi Antenna angle iron fastened to the pole as high as 2 meters outside the house in Kampung Parit Raja Darat. Antenna is directed 125o East to Johor Baharu. The angle of elevation of the antenna is determined by an equation below and refer to Figure 4.2. it only takes a loss due to propagation and absorption in meteorites. It involves analysis of meteor Fresnel zone. Antenna transmitter and receiver is considered lost. The angle between the axis of propagation of the meteor and the plane is taken as β .

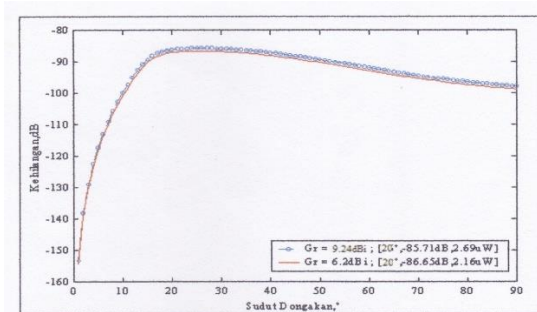


Figure 4.14 Loss Compared Angle Tilt

Output antenna is inserted into the pre amplifier using wires RG58U. Pre-amplifier connected to commercial radio. Radio output so put enter the sound card on your computer that contains software spectrogram. Software spectrogram is a plot of the frequency of the power spectrum as a function of time. It analyzes the format shift code modulation (PCM) digital audio to produce the plot. This allows the classification of sound is made, frequency analysis was performed by the Fast Fourier transfer

(FFT) allowing the frequency resolution and display data in optimizing.

Observations and Results

Observations were carried out early to see changes in the received signal. On 02 August 2017 the first observations made where it's not a peak time schedule or time range in 2017. The meteor shower observation found no signal is found. But while there are objects that reflect the observed signal. Having studied the possibilities available to other objects that pass light aircraft which can reflect signals. Results of observations on 02 August 2017 are as diagrams 4:16

Then again the observations made during the peak hours on 12 August 2017 in which it found no trace of the meteor is detected. Figure successfully in place and it is kind of Perseids meteor. 4:15 reflection diagram of the signal obtained very clear where the tail of a meteor (burst) has looked at a frequency between 1 kHz to 2 kHz in the range of 8 seconds before it disappeared. Signal reception has also been able to receive radio wave signals from the receiver of Perlis FM 102.9MHz transmitter station for 8 seconds before it disappeared.

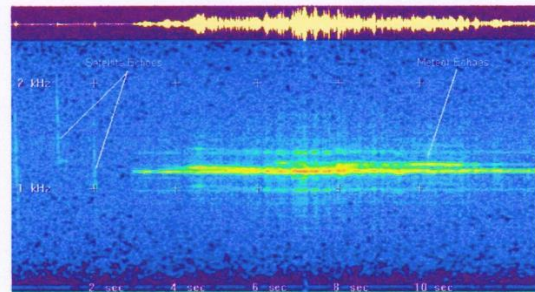


Figure 4.15: the results obtained from the actual display of Perseids meteor

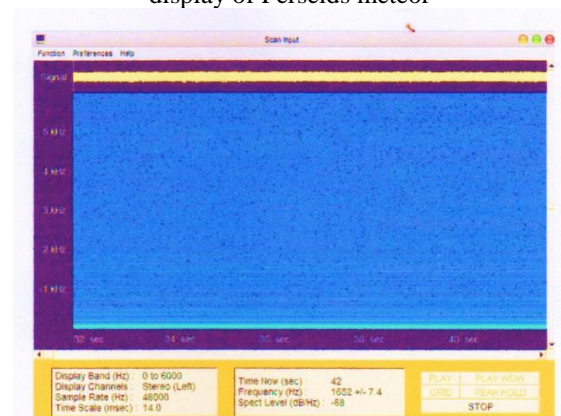


Figure 4.16: Display of the results of observations at 2230 local time, 02 August 2017

Conclusion

Construction of radio signal reception system via meteor scatter communications medium involves the design and testing of 6 elements Yagi antenna and pre-amplifier exceeds 10dB. The measurement results found characteristics of the antenna and pre-amplifier is not like in the simulation. However, it still meets specifications. In addition a number of assumptions and mathematical models used to analyze the characteristic signal. Radio signal receiver system via meteor scatter communications successfully completed the theoretical and practical, but it requires a certain time based on the schedule to successfully observe meteor showers. In accordance with the objectives of the study, which requires to build and create a system that can identify meteor activity in areas near the equator, develop appropriate equipment in the frequency range of VHF and choose the appropriate software to analyze is achieved. All problems concentrated expected to occur have been addressed at the end of the study. Apart from the new knowledge and experience is invaluable in assessing the meteor activity was obtained and will continue in times to come.

- Hu, Z., Shen, Z., Wu, W., & Lu, J. (2015). Low-Profile Top-Hat Monopole Yagi Antenna for End-Fire Radiation. *IEEE Transactions on Antennas and Propagation*, 63(7), 2851–2857. doi:10.1109/tap.2015.2427853
- Juan, L., Guang, F., Lin, Y., & Demin, F. (2007). Optimization and Application of the Yagi-Uda Antenna for Meteor Burst Communication. 2007 International Symposium on Microwave, Antenna, Propagation and EMC Technologies for Wireless Communications. doi:10.1109/mape.2007.4393710
- Jurgen Rendtel. (2017). 2017 Meteor Shower Calender. Retrieved from <https://www.imo.net/files/meteor-shower/cal2017.pdf>
- Lesanu, C. E., Done, A., Căilean, A. M., & Graur, A. (2018). Vertical polarized antennas for Low-VHF radio meteor detection. In 2018 International Conference on Development and Application Systems (DAS) (pp. 93-98). IEEE.
- Pearce, N., & Duncan, K. J. (2021, March). Simulation and Comparison of Weak-Signal VHF Propagation. In SoutheastCon 2021 (pp. 1-5). IEEE.
- Peter Jenniskens. (2017). Meteor Showers in Review. *Planetary and Space Science* (2017), <http://dx.doi.org/10.1016/j.pss.2017.01.008>
- Reddy, K. C., & Premkumar, B. (2018). Meteor head and terminal flare echoes observed with the Gadanki MST radar. *Journal of Atmospheric and Solar-Terrestrial Physics*. doi:10.1016/j.jastp.2018.11.006
- Sciancalepore, S., Oligeri, G., & Di Pietro, R. (2018, May). Shooting to the stars: secure location verification via meteor burst communications. In 2018 IEEE Conference on Communications and Network Security (CNS) (pp. 1-9). IEEE.
- Straub, G. J. (2017). Radio Wave Propagation. In *The RF Transmission Systems Handbook* (pp. 15-1). CRC Press.
- Sulimov, A. I. (2017). On possibility of using of measurements of random polarization of radio reflections from meteor trails for generating shared encryption keys. In 2017 Radiation and Scattering of Electromagnetic Waves (RSEMW) (pp. 146-149). IEEE.
- Sulimov, A. I., Karpov, A. V., Lapshina, I. R., & Khuzyashev, R. G. (2017). Analysis and simulation of channel nonreciprocity in meteor-

References:

- burst communications. *IEEE Transactions on Antennas and Propagation*, 65(4), 2009-2019.
- Urco, J. M., Chau, J. L., Weber, T., Vierinen, J. P., & Volz, R. (2019). Sparse signal recovery in MIMO specular meteor radars with waveform diversity. *IEEE Transactions on Geoscience and Remote Sensing*, 57(12), 10088-10098.
- Wakabayashi, R. (2020). Practice of Meteor Burst Communication. In *Analyzing the Physics of Radio Telescopes and Radio Astronomy* (pp. 213-228). IGI Global.
- Oetting, J. (1980). An Analysis of Meteor Burst Communications for Military Applications. *IEEE Transactions on Communications*, 28(9), 1591–1601. doi:10.1109/tcom.1980.1094849
- Cannon, P. S., & Reed, A. P. C. (1987). The evolution of meteor burst communications systems. *Journal of the Institution of Electronic and Radio Engineers*, 57(3), 101. doi:10.1049/jiere.1987.0043
- Yavuz, D. (1990). Meteor burst communications. *IEEE Communications Magazine*, 28(9), 40–48. doi:10.1109/35.57696
- Glover, I. A. (1991). Meteor burst propagation. *Electronics & Communications Engineering Journal*, 3(4), 185. doi:10.1049/ecej:19910032
- Ince, A. (1980). Spatial Properties of Meteor-Burst Propagation. *IEEE Transactions on Communications*, 28(6), 841–849. doi:10.1109/tcom.1980.1094739
- H. (2017). PERLISFM - our-frequency. Retrieved February 15, 2017, from <https://perlisfm.rtm.gov.my/our-frequency>
- Jayaram, A. S. (2021). New Theorem on Triangles-more Generalized Than Pythagoras Theorem. *Int. J. Math. And Appl.*, 9(2), 105-110.
- McKinley, D. W. R. (1961). *Meteor science and engineering*. New York.
- Yagi-Uda.com. (2011). Yagi-Uda antenna. Retrieved September 16, 2021, from <http://yagi-uda.com/>
- Jones, E. A., & Joines, W. T. (1997). Design of Yagi-Uda antennas using genetic algorithms. *IEEE Transactions on Antennas and Propagation*, 45(9), 1386–1392. doi:10.1109/8.623128
- Reddy, M. P. (2018). Directional Yagi Uda antenna for VHF applications. *International Journal of Advancements in Technology*, 9(3), 1-3.
- Stutzman, W. L., & Thiele, G. A. (2012). *Antenna theory and design*. John Wiley & Sons.
- Silver, S. (Ed.). (1984). *Microwave antenna theory and design* (No. 19). Iet.
- Balanis, C. A. (1992). *Antenna theory: A review*. *Proceedings of the IEEE*, 80(1), 7-23.
- Pozar, D. M. (2000). *Microwave and RF design of wireless systems*. John Wiley & Sons.